DOI:10.1158/1078-0432.CCR-10-2291

Ser36) leads to ubiquitination of IκB and subsequent proteasome-mediated degradation in the canonical NF-κB induction pathway (17). A dominant-negative mutant of IκBα, named IκBαM, has been engineered to be protected from phosphorylation and degradation. The introduction of this mutant form tightly represses the nuclear translocation and DNA binding of NF-κB (18). To elucidate the role of NF-κB in *KRAS*-induced endometrial carcinogenesis, we established cell lines with disabled NF-κB function by introducing IκBαM into EM-E6/E7/TERT/RAS cells. We first confirmed the inhibitory effect of this mutant, using the luciferase reporter assay. As shown in Figure 3A, the introduction of IκBαM significantly repressed the ability of NF-κB to activate the target promoters. We also confirmed that ERK activity was not affected by the introduction of IκBαM by Western blot analyses (Fig. 3B). Transformed phenotypes of this transfectant were evaluated by cell growth *in vitro* and the soft agar colony formation assay, tumor formation assay in nude mice, and Matrigel invasion assay. Under normal serum conditions, there was no significant increase in exponential growth rate by the introduction of IκBαM (data not shown). However, in low-serum conditions with 0.5% FBS, cells with overexpressed IκBαM exhibited decreased growth rate (Fig. 4A). We also observed that anchorage-independent growth in soft agar was almost completely abolished in these mutant cells (Fig. 4B). Furthermore, these cells completely lost their tumorigenic potential in mice (Fig. 4C). Similarly, their invasive ability significantly decreased, as evaluated by the Matrigel invasion assay (Fig. 4D). These findings indicate the crucial roles of NF-κB in *KRAS*-mediated endometrial carcinogenesis.

NF-κB activation by oncogenic *KRAS* is IKK dependent but independent of p65 phosphorylation or IκBα degradation/dissociation

We next sought to identify the molecular mechanisms of NF-κB activation by oncogenic *KRAS*. We first tested whether IKK signaling involves this activation. EM-E6/E7/TERT/RAS cells were treated with or without the IKK inhibitor X, the molecule known to inactivate IKKβ and IKKα. As shown in Figure 5A, the addition of IKK inhibitors largely inhibited the activity of NF-κB–responsive promoter in *KRAS*-introduced cells but not vector cells, indicating that this activation was IKK dependent.

Recent studies have focused on IκB subtype regulation (19) or p65 nuclear modification which can affect DNA binding and interactions with coactivators and corepressors (20, 21). Thus, we compared the basal expression levels of IκB subtypes or p65 modification between EM-E6/E7/TERT/vec and EM-E6/E7/TERT/RAS cells. As shown in Figure 5B, the expression levels of IκBα, β, ε, and p105 and those of phospho-p65 at Ser276, 529, and 536 were basically equivalent in both cells except p100. These findings suggest that IκB subtype regulation or p65 nuclear modification does not significantly contribute to *KRAS*-induced NF-κB activation during endometrial carcinogenesis.

One potential mechanism of NF-κB activation includes the degradation of IκB by its ubiquitination. Therefore, we further evaluated the change in degradation rate of IκBα by Western blot analyses, using the protein synthesis inhibitor emetine. As expected, the treatment of cells with emetine resulted in the decreased expression of IκBα in both EM-E6/E7/TERT/vec and EM-E6/E7/TERT/RAS cells but not in

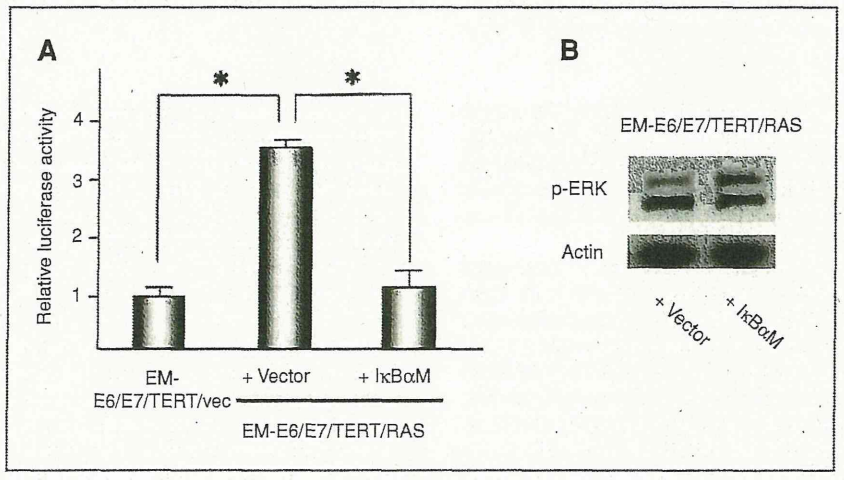

Figure 3. Introduction of IκBαM effectively inhibits NF-κB activity in transformed endometrial epithelial cells. EM-E6/E7/TERT/RAS cells were stably overexpressed with IκBαM lacking phosphorylation sites essential for its degradation, thereby becoming stable against degradation signals. Eventually, these transfectants were expected to have disabled NF-κB by IκB activity. To confirm the *in vivo* function of NF-κB in these cells, luciferase assays were done, in which EM-E6/E7/TERT/RAS cells or the vector control EM-E6/E7/TERT/vec cells were transfected with reporter plasmids containing the NF-κB–responsive elements and the luciferase assays were conducted. A, relative luciferase activities are shown as the mean values of 3 independent experiments, in which those of E6/E7/TERT/vec cells were normalized to 1.0. Bars, SD. *, $P < 0.05$. B, states of the RAF-ERK pathway were compared between EM-E6/E7/TERT/RAS cells transfected with IκBαM and the vector control cells, examining the phosphorylated ERK expression by Western blot analysis.

DOI:10.1158/1078-0432.CCR-10-2291

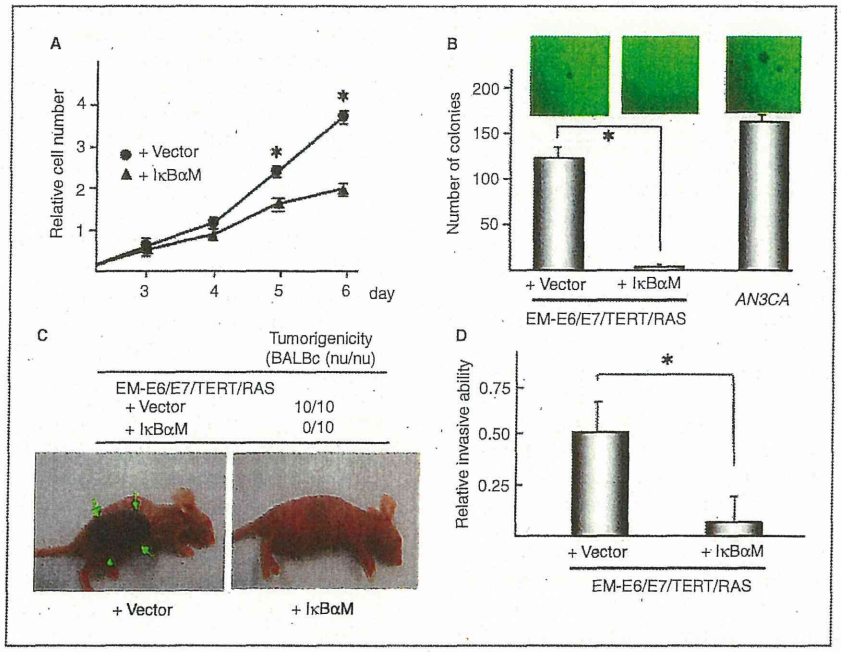

Figure 4. Transforming activity of oncogenic *KRAS* is disturbed by inhibiting NF-κB activity in endometrial epithelial cells. Transformed phenotypes of EM-E6/E7/TERT/RAS cells overexpressed with IκBαM were evaluated by various experiments. A, cell growth assay in a low-serum condition. The growth curve is shown in which EM-E6/E7/TERT/RAS cells transfected with or without IκBαM were cultured at a low-serum concentration with 0.5% FBS. Bars, SD. *, statistically significant decrease ($P < 0.05$) in the number of EM-E6/E7/TERT/RAS cells overexpressed with IκBαM compared with the number of vector control cells on days 5 and 6. B, soft agar colony formation assay. A total of 10,000 cells were seeded on soft agar in 6-cm dishes and colonies with a diameter of more than 0.05 mm 4 weeks after seeding were counted. Bars, SD. *, $P < 0.01$. C, nude mice xenograft experiment. A total of 10^7 cells of EM-E6/E7/TERT/RAS with IκBαM or control vector were inoculated subcutaneously into the right trunk of immunodeficient mice. Tumor formation was monitored for 8 weeks after inoculation. Breast cancer AN3CA cells were used as a positive control for colony formation. D, Matrigel invasion assay. EM-E6/E7/TERT/RAS cells with IκBαM or control vector were suspended in the upper wells of Matrigel chambers at 250,000 cells/chamber. After incubation, cells on the upper surface of the membrane were removed, and the cells that had migrated through the membrane to the lower surface were counted microscopically. The numbers are shown as relative invasive ability. Bars, SD. *, $P < 0.05$.

cells with overexpressed IκBαM lacking phosphorylation sites responsible for degradation (Fig. 5C). However, the degradation ratio was equivalent in EM-E6/E7/TERT/vec and EM-E6/E7/TERT/RAS cells. These results show that the activation of NF-κB by oncogenic *KRAS* is not due to accelerated degradation of IκBα.

The remaining possibility of activation mechanism might be an enhanced dissociation of p65 with IκBα (22). We tested this possibility by immunoprecipitation with p65 antibody, followed by the Western blot analysis with IκBα antibody, using extracts from EM-E6/E7/TERT/vec and EM-E6/E7/TERT/RAS cells. As shown in Figure 5D, the ratio of IκBα associated with p65 was similar between EM-E6/E7/TERT/vec and EM-E6/E7/TERT/RAS cells, denying the involvement of enhanced dissociation of p65 with IκBα.

Discussion

Using an *in vitro* carcinogenesis model with human endometrial epithelial cells, we first investigated the status of 2 major signaling pathways, the RAF-MEK-ERK and PI3K-Akt pathways, downstream of Ras. As expected, phosphorylated ERK expression significantly increased in EM-E6/E7/TERT/RAS cells (Fig. 1A). In contrast, phosphorylated Akt expression was not detected in both EM-E6/E7/TERT/vec and EM-E6/E7/TERT/RAS cells (Fig. 1B). However, the introduction of a constitutively active form of MEK, mimicking the activated RAF-MEK-ERK pathway, failed to show transformed phenotypes. Thus, activation of ERK alone was not sufficient to transform EM-E6/E7/TERT cells. There are several reports showing that constitutive activation of MEK successfully transformed rodent epithelial cells (23–26). In contrast, Boehm and colleagues showed that the introduction of a constitutively active form of MEK failed to transform immortalized human embryonic kidney epithelial cells (27). These results together with our results suggest that activation of the MEK-ERK pathway alone may not be sufficient to transform human epithelial cells and that the activation of other oncogenic pathways is required. Thus, we sought novel effectors involved in KRAS-mediated endometrial carcinogenesis.

DOI:10.1158/1078-0432.CCR-10-2291

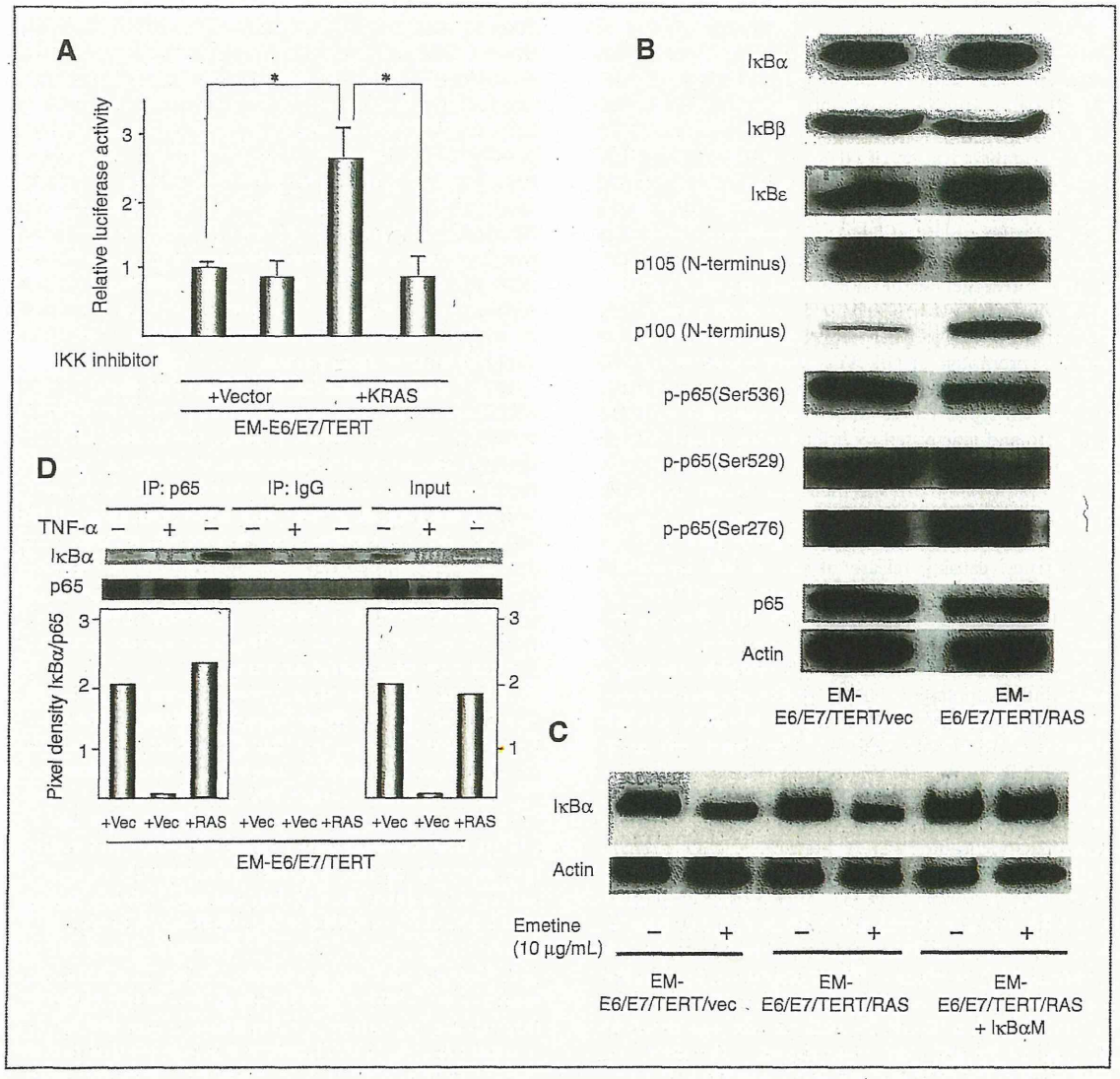

Figure 5. *KRAS*-induced activation of NF-κB in endometrial carcinogenesis is IKK dependent but not on known canonical pathways. A, IKK dependence of NF-κB activation. EM-E6/E7/TERT/vec cells or EM-E6/E7/TERT/RAS cells were transfected with reporter plasmids containing the NF-κB–responsive elements and were incubated with or without 5 μmol/L of IKK inhibitor X. Luciferase assays were carried out after 48 hours of incubation. Relative luciferase activities are shown as the mean values of 3 independent experiments, in which those of E6/E7/TERT/vec cells were normalized to 1.0. Bars, SD. *, $P < 0.05$. B, expression levels of IκB family proteins and phosphorylated p65 in *KRAS*-introduced cells. Whole-cell extracts of EM-E6/E7/TERT/vec cells or EM-E6/E7/TERT/RAS cells were subjected to the Western blot analysis, and the levels of expression in each factor are compared. C, change in IκBα turnover rate was compared between cells with or without oncogenic *KRAS*. EM-E6/E7/TERT/RAS cells or EM-E6/E7/TERT/vec cells were treated with or without 10 μg/mL of emetine and the whole-cell extracts were subjected to the Western blot analysis for IκBαM. As a control, EM-E6/E7/TERT cells with overexpressed IκBαM were used, in which IκBα level is stable even in the presence of emetine due to the lack of the specific phosphorylation site essential for degradation. D, change in dissociation rate of p65 with IκBα was compared between cells with or without oncogenic *KRAS*. Immunoprecipitation (IP) was carried out with antibodies against p65 or control IgG, using whole-cell lysates from EM-E6/E7/TERT/vec or EM-E6/E7/TERT/RAS cells. TNF-α (20 ng/mL for 5 minutes) stimulation was carried out in vector (Vec) cells to facilitate the degradation of IκBα, used as a positive control of degradation status. Western blot analysis was subsequently carried out on immunoprecipitants with antibodies to p65 or IκBα. The pixel densities of IκBα and p65 Western blots were quantified using NIH Scion software. Graph represents the relative pixel density of IκBα normalized to p65 levels in each sample.

DOI:10.1158/1078-0432.CCR-10-2291

NF-κB transcriptional factor is a putative effector of Ras-mediated transformation (8–10). We showed that oncogenic *KRAS* enhanced the NF-κB binding to its responsive elements and facilitated the transactivation of the target promoters. The introduction of IκBαM successfully inhibited transactivation of NF-κB without affecting ERK activity, and we found that such inhibition completely abrogated the anchorage-independent growth and tumor-forming ability of EM-E6/E7/TERT/RAS cells, suggesting a major contribution of NF-κB activity to *KRAS*-induced carcinogenesis of endometrial epithelial cells.

What is the molecular mechanism of NF-κB activation in *KRAS*-induced endometrial carcinogenesis? The transactivation of promoters by NF-κB is directly controlled by its nuclear translocation and its modification in the nucleus. In most cell types, NF-κB dimers are sequestered in the cytoplasm and inactivated by IκB proteins, which bind to the NF-κB and mask the nuclear localization signal (28). The phosphorylation of a specific serine residue, Ser32/36, in IκBα by the upstream regulators such as IKK results in polyubiquitination and subsequent degradation by 26 S proteasomes, causing release of the NF-κB dimer and promoting its translocation to the nucleus, activating various κB-responsive gene expressions (29, 30). Thus, we first tested the involvement of IKK in the activation. The treatment of EM-E6/E7/TERT/RAS cells with the IKK inhibitor X significantly suppressed NF-κB transcriptional activity, confirming that *KRAS*-induced NF-κB activation was IKK dependent. We further examined the basal expression levels of IκB family proteins in the presence or absence of oncogenic *KRAS* and found that the expression levels of IκB proteins, including IκBα, β, ε, and p105, were not affected by oncogenic *KRAS*. Expression of p100 protein, which is a member of the IκB protein family and a precursor of NF-κB subunit p52 (31), increased in EM-E6/E7/TERT/RAS cells. This is probably because the p100 promoter contains a κB site (32). We do not consider that this phenomenon is involved in NF-κB activation, because the increased expression of p100 may inhibit NF-κB activity but never activates NF-κB. In addition, the expression of p52 was unchanged (data not shown). Therefore, we speculate that the p100/p52 subunit is not likely to participate in NF-κB activation by oncogenic *KRAS*. Furthermore, we focused on the modification of the NF-κB subunit itself. Nuclear NF-κB modification, especially p65/RelA subunit modification, has been investigated and found to affect DNA binding and interactions with coactivators and corepressors and the termination of the NF-κB response (33). These modifications include phosphorylation of Ser536 and Ser529 in the C-terminal transactivation domains and Ser276 in the Rel homology domain (17, 34–36). However, the expression of phosphorylated p65 was not elevated in the *KRAS*-introduced cells. We further confirmed the possibility of increased IκB degradation that might result in NF-κB activation. The IκB turnover assay with protein synthesis inhibitor revealed that the turnover was not accelerated by oncogenic *KRAS*, again denying the possibility as an activation mechanism. Recently proven additional mechanisms of NF-κB activation is a dissociation of IκB from p65 in the absence of IκB degradation (22, 37). We examined the interaction of IκBα and p65 by immunoprecipitation. The expression levels of IκBα attached to p65 was, however, equivalent between EM-E6/E7/TERT/vec and EM-E6/E7/TERT/RAS cells, showing that such dissociation is not involved in *KRAS*-mediated NF-κB activation. Thus, we concluded that *KRAS*-induced activation of NF-κB during endometrial carcinogenesis is IKK dependent but not on known canonical pathways. Identification of such unknown mechanisms is needed using our model for understanding not only of the activation mechanisms of NF-κB but also of the carcinogenesis of endometrium.

So far, only one study has addressed *KRAS* mutation and NF-κB activation in endometrial cancer (38). This report examined surgically resected cancer tissues and reported the high frequency of nuclear location of NF-κB families. However, no correlation was found between the nuclear immunostaining of NF-κB and *KRAS* mutation. These findings do not conflict with our results, because their analyses were carried out using specimens of progressive cancers and not samples at the stage of cancer initiation or development, in which network of etiologic factors might be modified because of acquired genetic alterations during the late stage of cancer development.

This study may provide a clinical implication for NF-κB as a novel molecular target for cancer chemoprevention of the endometrium. Accumulating evidence has clarified chemopreventive effects of anti-inflammatory agents such as aspirin or other nonsteroidal anti-inflammatory drugs on various cancer types partially via inhibition of NF-κB (39, 40). As for endometrial cancer, Moysich and colleagues reported the risk reduction by regular use of aspirin among obese women (41). Interestingly, multiple signaling pathways, including PTEN-PI3K-Akt pathway, are known to activate NF-κB in endometrial cancer cells (42). Loss of function mutation in *PTEN* and activating mutation in *PIK3CA* are putative activator of NF-κB through Akt expression in endometrial cancer and in the precursor lesions (43). Therefore, it is possible that NF-κB plays a role in endometrial carcinogenesis via various pathways other than *KRAS*-driven pathways, giving light to the potential role of NF-κB inhibitors in preventing endometrial carcinogenesis.

In summary, we for the first time show that the activation of NF-κB is a novel target of oncogenic *KRAS* in endometrial carcinogenesis. Blockade of NF-κB activity led to effective inhibition of transformed phenotypes of endometrial cells. These findings may add the novel information on the molecular pathway of endometrial carcinogenesis, implying the potential utility of NF-κB inhibitors for endometrial cancer chemoprevention, especially with *KRAS* mutation.

Disclosure of Potential Conflicts of Interest

The authors declare no conflict of interest.

DOI:10.1158/1078-0432.CCR-10-2291

Grant Support

This study was supported by a grant-in-aid for Scientific Research from the Japan Society for the Promotion of Science (JSPS) and the Megumi Medical Foundation of Kanazawa University.

The costs of publication of this article were defrayed in part by the payment of page charges. This article must therefore be hereby marked *advertisement* in accordance with 18 U.S.C. Section 1734 solely to indicate this fact.

Received August 26, 2010; revised December 17, 2010; accepted December 29, 2010; published online March 16, 2011.

References

1. Hecht JL, Mutter GL. Molecular and pathologic aspects of endometrial carcinogenesis. J Clin Oncol 2006;24:4783–91.
2. Inoue M. Current molecular aspects of the carcinogenesis of the uterine endometrium. Int J Gynecol Cancer 2001;11:339–48.
3. Enomoto T, Inoue M, Perantoni AO, Buzard GS, Miki H, Tanizawa O, et al. K-ras activation in premalignant and malignant epithelial lesions of the human uterus. Cancer Res 1991;51:5308–14.
4. Mutter GL. K-ras mutations appear in the premalignant phase of both microsatellite stable and unstable endometrial carcinogenesis. Mol Pathol 1999;52:257–62.
5. Shields JM, Pruitt K, McFall A, Shaub A, Der CJ. Understanding Ras: "it ain't over 'til it's over." Trends Cell Biol 2000;10:147–54.
6. Kyo S, Nakamura M, Kiyono T, Maida Y, Kanaya T, Tanaka M, et al. Successful immortalization of endometrial glandular cells with normal structural and functional characteristics. Am J Pathol 2003;163:2259–69.
7. Mizumoto Y, Kyo S, Ohno S, Hashimoto M, Nakamura M, Maida Y, et al. Creation of tumorigenic human endometrial epithelial cells with intact chromosomes by introducing defined genetic elements. Oncogene 2006;25:5673–82.
8. Bassères DS, Baldwin AS. Nuclear factor-kappaB and inhibitor of kappaB kinase pathways in oncogenic initiation and progression. Oncogene 2006;25:6817–30.
9. Hanson JL, Hawke NA, Kashatus D, Baldwin AS. The nuclear factor kappaB subunits RelA/p65 and c-Rel potentiate but are not required for Ras-induced cellular transformation. Cancer Res 2004;64:7248–55.
10. Arsura M, Mercurio F, Oliver AL, Thorgeirsson SS, Sonenshein GE. Role of the IkappaB kinase complex in oncogenic Ras- and Raf-mediated transformation of rat liver epithelial cells. Mol Cell Biol 2000;20:5381–91.
11. Millán O, Ballester A, Castrillo A, Oliva JL, Través PG, Rojas JM, et al. H-Ras-specific activation of NF-kappaB protects NIH 3T3 cells against stimulus-dependent apoptosis. Oncogene 2003;22:477–83.
12. Schreiber E, Matthias P, Müller MM, Schaffner W. Rapid detection of octamer binding proteins with "mini-extracts," prepared from a small number of cells. Nucleic Acids Res 1989;17:6419.
13. Gopalbhai K, Jansen G, Beauregard G, Whiteway M, Dumas F, Wu C, et al. Negative regulation of MAPKK by phosphorylation of a conserved serine residue equivalent to Ser212 of MEK1. J Biol Chem 2003;278:8118–25.
14. Narisawa-Saito M, Yoshimatsu Y, Ohno S, Yugawa T, Egawa N, Fujita M, et al. An *in vitro* multistep carcinogenesis model for human cervical cancer. Cancer Res 2008;68:5699–705.
15. Sato H, Takino T, Okada Y, Cao J, Shinagawa A, Yamamoto E, et al. A matrix metalloproteinase expressed on the surface of invasive tumour cells. Nature 1994;370:61–5.
16. Brunet A, Pagès G, Pouysségur J. Constitutively active mutants of MAP kinase kinase (MEK1) induce growth factor-relaxation and oncogenicity when expressed in fibroblasts. Oncogene 1994;9:3379–87.
17. DiDonato J, Mercurio F, Rosette C, Wu-Li J, Suyang H, Ghosh S, et al. Mapping of the inducible IkappaB phosphorylation sites that signal its ubiquitination and degradation. Mol Cell Biol 1996;16:1295–304.
18. Wang CY, Mayo MW, Baldwin AS Jr. TNF- and cancer therapy-induced apoptosis: potentiation by inhibition of NF-kappaB. Science 1996;274:784–7.
19. Hayden MS, Ghosh S. Signaling of NF-kappaB. Genes Dev 2004;18:2195–224.
20. Vermeulen L, De Wilde G, Van Damme P, Vanden Berghe W, Haegeman G. Transcriptional activation of the NF-kappaB p65 subunit by mitogen- and stress-activated protein kinase-1 (MSK1). EMBO J 2003;22:1313–24.
21. Chen LF, Williams SA, Mu Y, Nakano H, Duerr JM, Buckbinder L, et al. NF-kappaB RelA phosphorylation regulates RelA acetylation. Mol Cell Biol 2005;25:7966–75.
22. Sitcheran R, Comb WC, Cogswell PC, Baldwin AS. Essential role for epidermal growth factor receptor in glutamate receptor signaling to NF-kappaB. Mol Cell Biol 2008;28:5061–70.
23. Haluska FG, Tsao H, Wu H, Haluska FS, Lazar A, Goel V. Genetic alterations in signaling pathways in melanoma. Clin Cancer Res 2006;12:2301s–7s.
24. Deerberg F, Kaspareit J. Endometrial carcinoma in BD II/Han rats: model of a spontaneous hormone-dependent tumor. J Natl Cancer Inst 1987;78:1245–51.
25. Komatsu K, Buchanan FG, Otaka M, Jin M, Odashima M, Horikawa Y, et al. Gene expression profiling following constitutive activation of MEK1 and transformation of rat intestinal epithelial cells. Mol Cancer 2006;5:63.
26. Pinkas J, Leder P. MEK1 signaling mediates transformation and metastasis of EpH4 mammary epithelial cells independent of an epithelial to mesenchymal transition. Cancer Res 2002;62:4781–90.
27. Boehm JS, Zhao JJ, Yao J, Kim SY, Firestein R, Dunn IF, et al. Integrative genomic approaches identify IKBKE as a breast cancer oncogene. Cell 2007;129:1065–79.
28. Huxford T, Huang DB, Malek S, Ghosh G. The crystal structure of the IkappaBalpha/NF-kappaB complex reveals mechanisms of NF-kappaB inactivation. Cell 1998;95:759–70.
29. Chen Z, Hagler J, Palombella VJ, Melandri F, Scherer D, Ballard D, et al. Signal-induced site-specific phosphorylation targets I kappa B alpha to the ubiquitin-proteasome pathway. Genes Dev 1995;9:1586–97.
30. Scherer DC, Brockman JA, Chen Z, Maniatis T, Ballard DW. Signal-induced degradation of I kappa B alpha requires site-specific ubiquitination. Proc Natl Acad Sci U S A 1995;92:11259–63.
31. Dejardin E. The alternative NF-kappaB pathway from biochemistry to biology: pitfalls and promises for future drug development. Biochem Pharmacol 2006;72:1161–79.
32. Lombardi L, Ciana P, Cappellini C, Trecca D, Guerrini L, Migliazza A, et al. Structural and functional characterization of the promoter regions of the NFKB2 gene. Nucleic Acids Res 1995;23:2328–36.
33. Perkins ND. Post-translational modifications regulating the activity and function of the nuclear factor kappa B pathway. Oncogene 2006;25:6717–30.
34. Sakurai H, Chiba H, Miyoshi H, Sugita T, Toriumi W. IkappaB kinases phosphorylate NF-kappaB p65 subunit on serine 536 in the transactivation domain. J Biol Chem 1999;274:30353–6.
35. Zhong H, Voll RE, Ghosh S. Phosphorylation of NF-kappa B p65 by PKA stimulates transcriptional activity by promoting a novel bivalent interaction with the coactivator CBP/p300. Mol Cell 1998;1:661–71.
36. Wang D, Westerheide SD, Hanson JL, Baldwin AS Jr. Tumor necrosis factor alpha-induced phosphorylation of RelA/p65 on Ser529 is controlled by casein kinase II. J Biol Chem 2000;275:32592–7.
37. Mabuchi R, Sasazuki T, Shirasawa S. Mapping of the critical region of mitogene-inducible gene-6 for NF-kappaB activation. Oncol Rep 2005;13:473–6.

DOI:10.1158/1078-0432.CCR-10-2291

38. Pallares J, Martínez-Guitarte JL, Dolcet X, Llobet D, Rue M, Palacios J, et al. Abnormalities in the NF-kappaB family and related proteins in endometrial carcinoma. J Pathol 2004;204:569–77.
39. Cuzick J, Otto F, Baron JA, Brown PH, Burn J, Greenwald P, et al. Aspirin and non-steroidal anti-inflammatory drugs for cancer prevention: an international consensus statement. Lancet Oncol 2009;10:501–7.
40. Zhang Z, Rigas B. NF-kappaB, inflammation and pancreatic carcinogenesis: NF-kappaB as a chemoprevention target. Int J Oncol 2006;29:185–92.
41. Moysich KB, Baker JA, Rodabaugh KJ, Villella JA. Regular analgesic use and risk of endometrial cancer. Cancer Epidemiol Biomarkers Prev 2005;14:2923–8.
42. St-Germain ME, Gagnon V, Parent S, Asselin E. Regulation of COX-2 protein expression by Akt in endometrial cancer cells is mediated through NF-kappaB/IkappaB pathway. Mol Cancer 2004;3:7.
43. Hayes MP, Wang H, Esponal-Witter R. PIK3CA and PTEN mutation in uterine endometrioid carcinoma and complex hyperplasia. Clin Cancer Res 2006;12:5932–5.

Open

Cancer Gene Therapy (2011) 18, 77–86

www.nature.com/cgt

ORIGINAL ARTICLE

Carrier cell-based delivery of replication-competent HSV-1 mutants enhances antitumor effect for ovarian cancer

S Fujiwara[1,2], A Nawa[1], C Luo[2], M Kamakura[2], F Goshima[2], C Kondo[3], T Kiyono[4], F Kikkawa[1] and Y Nishiyama[2]

[1]*Department of Obstetrics and Gynecology, Nagoya University Graduate School of Medicine, 65 Tsurumai-cho, Nagoya, Japan;* [2]*Department of Virology, Nagoya University Graduate School of Medicine, 65 Tsurumai-cho, Nagoya, Japan;* [3]*Department of Biochemistry, School of Dentistry, Aichi-Gakuin University, Nagoya, Japan and* [4]*Virology Division, National Cancer Center Research Institute, Tokyo, Japan*

Oncolytic viruses capable of tumor-selective replication and cytolysis have shown early promise as cancer therapeutics. We have developed replication-competent attenuated herpes simplex virus type 1 (HSV-1) mutants, named HF10 and Hh101, which have been evaluated for their oncolytic activities. However, the host immune system remains a significant obstacle to effective intraperitoneal administration of these viruses in the clinical setting. In this study, we investigated the use of these HSV-1 mutants as oncolytic agents against ovarian cancer and the use of human peritoneal mesothelial cells (MCs) as carrier cells for intraperitoneal therapy. MCs were efficiently infected with HSV-1 mutants, and MCs loaded with HSV-1 mutants caused cell killing adequately when cocultured with cancer cells in the presence or absence of HSV antibodies. In a mouse xenograft model of ovarian cancer, the injection of infected carrier cells led to a significant reduction of tumor volume and prolonged survival in comparison with the injection of virus alone. Our results indicate that replication-competent attenuated HSV-1 exerts a potent oncolytic effect on ovarian cancer, which may be further enhanced by the utilization of a carrier cell delivery system, based on amplification of viral load and possibly on avoidance of neutralizing antibodies.
Cancer Gene Therapy (2011) **18,** 77–86; doi:10.1038/cgt.2010.53; published online 1 October 2010

Keywords: oncolytic virotherapy; ovarian cancer; cell carriers; herpes simplex virus

Introduction

In Japan, 8000 cases of ovarian cancer are newly diagnosed and more than 4000 women die of this disease every year.[1] Ovarian cancer has a high fatality rate because of the lack of effective screening strategies and the absence of symptoms during the early stage of disease. Thus, most patients with ovarian cancer present with advanced-stage disease in conjunction with intraperitoneal carcinoma. Advanced epithelial ovarian cancer (EOC) is a highly chemosensitive solid tumor with good response rates to first-line chemotherapy. However, the majority of patients eventually relapse, and ultimately die of recurrent chemoresistant disease. Therefore, novel therapeutic approaches are required. EOC remains localized within the peritoneal cavity in a large proportion of patients, causing local morbidity and lethal complications.[2] Owing to its localized nature, EOC lends itself to intraperitoneal approaches to therapy, including gene therapy.

Oncolytic virotherapy is a promising anticancer therapy because efficient transduction and cancer cell-specific viral replication can boost therapeutic efficacy.[3–7] Therefore, oncolytic viral therapy is viewed as a new strategy for the treatment of advanced cancers. Many published reports describe the effectiveness of genetically engineered herpes simplex virus type 1 (HSV-1). HSV-1 has many advantages over other viruses for cancer gene therapy: (1) it has a broad host range and high efficiency of infection; (2) it has a large genomic capacity and can be engineered to deliver therapeutic transgenes;[8,9] and (3) it can be controlled by anti-herpetic drugs. Unlike retroviruses, the HSV genome does not integrate into the host genome, eliminating concerns of insertional mutagenesis. Clinical trials with several of these agents have been completed, with some efficacy. However, as the majority of those studies have relied on direct administration into target tissue, effective systemic viral delivery is required.

A major theoretical impediment to systemic application of HSV is pre-existing antiviral immunity. Almost all

Correspondence: Dr A Nawa, Department of Obstetrics and Gynecology, Nagoya University Graduate School of Medicine, 65 Tsurumai-cho, Showa-ku, Nagoya, Japan or Professor Y Nishiyama, Department of Virology, Nagoya University Graduate School of Medicine, 65 Tsurumai-cho, Showa-ku, Nagoya, Japan. E-mail: nawa@med.nagoya-u.ac.jp or ynishiya@med.nagoya-u.ac.jp
Received 22 November 2009; revised 23 April 2010; accepted 9 June 2010; published online 1 October 2010

individuals >30 years (about 80%) have circulating anti-HSV-1 antibodies in Japan.[10] Virus particles injected into the peritoneal cavity are vulnerable to inactivation by complement proteins, uptake by the reticuloendothelial system and neutralization by circulating antibodies.[11] Of these host defenses, antibodies are likely to be the most restrictive barrier to therapy, as they mediate a long-lasting state of immunity to repeated infections.[12] Several widely differing approaches aimed at protecting viral particles within the circulation and ensuring tumor delivery are currently the focus of intense research. For example, one possibility is modification of the viral coat,[13,14] although such technologies are technically challenging. In addition, cellular carriers could be used as Trojan Horse vehicles to shield oncolytic virus (OV) from neutralization following intraperitoneal administration, and act as *in situ* virus factories once arriving at the tumor site.[15,16]

In this study, we demonstrate that the molecular engineering of cellular carriers can increase their ability to support viral replication, promote direct cell-to-cell viral infection of the tumor, and shield oncolytic virus from neutralizing antibodies during delivery *in vitro*. Furthermore, we show the suitability of human peritoneal mesothelial cells (MCs) as a carrier system for delivery of HF10 and Hh101 to maximize the efficacy of oncolytic virus *in vivo*.

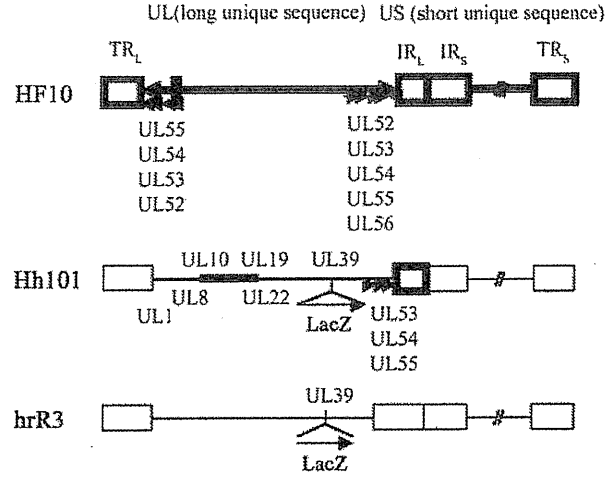

Figure 1 Models of the structures of herpes simplex virus type 1 (HSV-1) mutants. A schematic representation of the structure of the Hh101 and HF10 genomes. The locations of deletions and insertions in the genome of HF10 are shown. Expansions indicate the positions of genes within the deletion and insertion regions. Arrows indicate the position and orientation of genes within the expansions.

Materials and methods

Cell lines and viruses

Human ovarian cancer (SKOV3) cells were generously donated by Memorial Sloan-Kettering Cancer Research Laboratory. African green monkey kidney (Vero) cells were obtained from the Riken Cell Bank (Tsukuba, Ibaragi, Japan). SKOV3 cells were maintained in RPMI 1640 supplemented with 10% fetal calf serum and penicillin–streptomycin. Vero cells were grown in Eagle's minimal essential medium containing 10% calf serum and 1% penicillin–streptomycin. These cells were incubated at 37 °C in a humidified atmosphere of 5% CO_2.

hrR3, a ribonucleotide reductase (UL39)-deficient HSV-1 mutant, derived from the parental wild-type strain KOS, was kindly provided by Sandra K Weller (University of Connecticut Health Center, Farmington, CT). HF10 is a non-selected clone derived from HSV-1 strain HF and causes extensive cell membrane fusion in infected cells. Hh101 is a recombinant virus clone isolated from Vero cells co-infected with HF10 and hrR3 (Figure 1). The phenotypes of these viruses have been previously described.[17–19]

To visualize viruses *in vitro* and *in vivo*, the green fluorescent protein (*GFP*) gene was inserted into HF10 under control of the cytomegalovirus (CMV) promoter, in which UL43 was deleted. We named this virus HF-GFP.

Establishment and characterization of immortalized MCs

Human peritoneal MCs were isolated from surgical specimens of human omentum after obtaining consent from each patient, as described previously.[20] Briefly, small pieces of omentum were surgically resected under sterile conditions and were trypsinized at 37 °C for 30 min. The suspension was then passed through a 200-μm pore nylon mesh to remove undigested fragments, and centrifuged at 2000 r.p.m. for 5 min. The collected cells were cultured in RPMI 1640 supplemented with 10% fetal calf serum. In the subsequent experiments, cells were used during the second or third passage after primary culture.

Lentiviral vector plasmids were constructed by recombination using the Gateway system (Invitrogen, Carlsbad, CA). Briefly, hTERT, human cyclin D1 and human mutant Cdk4 (Cdk4R24C: an inhibitor resistant form of Cdk4) were first recombined into entry vectors by BP reaction (Invitrogen). Then these segments were recombined with a lentiviral vector, CSII-CMV-RfA, by LR reaction (Invitrogen) to generate CSII-CMV-hTERT, -cyclin D1 and -hCDK4R24C. The production of recombinant lentiviruses with the vesicular stomatitis virus G glycoprotein was as described previously.[21] Following the addition of recombinant viral fluid to MCs in the presence of 4 μg ml^{-1} polybrene, infected cells were selected in the presence of 250 μg ml^{-1} of G418, 0.5 μg ml^{-1} of puromycin, 3 μg ml^{-1} of blasticidin-S or 50 μg ml^{-1} of hygromycin-B. These cells are named human omentum mesothelial cells (HOmMCs). The study to establish immortalized MCs was approved by the local ethics committee and institutional review board of our hospital.

Anti-HSV-1 serum

Anti-HSV-1 serum was obtained from mice or guinea pigs by intravenous injection of HSV-1 grown in Vero cells. The neutralizing capacity of antiserum was determined by mixing about 100 plaque-forming units (PFU) of HSV-1 with serial dilutions of antiserum. The serum titer was

expressed as the dilution causing 50% plaque reduction: the neutralization titers of anti-HSV-1 mouse antiserum and anti-HSV-1 guinea pig antiserum were 1000 and 1600, respectively.

Viral replication assay

MCs or HOmMCs were plated on 35-mm dishes at a density of 3.7×10^5 cells per dish in 2 ml of the growth medium under standard conditions overnight. Cells were then infected with HF10 or Hh101 at multiplicities of infection (MOI) ranging between 0.03 and 3. To measure virus replication, cells were scraped from dishes at the indicated times, lysed by freeze–thaw and centrifuged at 3000 r.p.m. for 5 min. Viral titers were determined from the sample supernatants by plaque assay.

In vitro *delivery of HSV using MCs as carriers*

MCs were infected with Hh101 (MOI, 3) for 1 h at 37 °C; free virus was then removed and the cells were washed with phosphate-buffered saline (PBS) three times and resuspended in fresh medium. At 2 h after infection, the infected cells were trypsinized. The suspension was centrifuged at 1300 r.p.m. for 5 min at 4 °C. The collected cells were used as infected carrier cells.

SKOV3 cells were plated on 35-mm dishes at a density of 5.6×10^5 cells per dish in 2 ml of the growth medium. After 24 h, Hh101- (3×10^5 PFU) or Hh101-infected carrier cells (1×10^5 cells, MOI, 3) were added to the media, and we observed any resulting cytopathogenic effects (CPEs). At 24 h after infection, viral titers were determined from the sample supernatants by plaque assay.

In vitro *effects of anti-HSV-1 antiserum on HF-GFP*

HOmMCs were infected with HF-GFP (MOI, 3) for 1 h at 37 °C; free virus was then removed and the cells were washed with PBS three times and resuspended in fresh medium. At 2 h after infection, the infected cells were trypsinized. The suspension was then centrifuged at 1300 r.p.m. for 5 min at 4 °C. The collected cells were used as infected carrier cells.

SKOV3 cells were plated on 35-mm dishes. After 24 h, HF-GFP (10^5 PFU per dish) or HF-GFP-infected carrier cells (10^4 cells per dish) were added to the media with or without anti-HSV-1 mouse antiserum. At 24 h after infection, SKOV3 cells were photographed using the Leica (Wetglar, Germany) M205FA fluorescence stereomicroscope with a standard GFP filter set. At 30 h, SKOV3 cells were fixed with 4% formaldehyde and stained with 0.2% crystal violet solution. The number of plaques was counted under microscopy. The graphs (Figure 5e) were obtained from two independent experiments.

Animal studies

Animal studies were performed in accordance with guidelines issued by the Animal Center at Nagoya University School of Medicine. Female Balb/c slc nu/nu mice (5 to 6 weeks old) were purchased from Japan SLC (Hamamatsu, Japan). For surgical procedures, mice were anesthetized with an intraperitoneal injection of 7.2% chloral hydrate in sterile PBS (0.005 ml g^{-1} body weight).

Subcutaneous tumor model

To determine the therapeutic efficacy of HF10, we used a subcutaneous (s.c.) tumor model. SKOV3 cells were cultured and passaged twice *in vitro*, and 5×10^6 cells were injected s.c. into the flanks of 5-week-old nude mice. At 8 days after tumor challenge, when s.c. tumors were ~10–15 mm in diameter, mice were treated with intratumoral (i.t.) injection of HF10 (1×10^7 PFU). Animals in the first group were injected on days 8, 10 and 12. Animals in the second group were injected on days 8, 10, 12, 18, 20 and 22. Control mice were treated with i.t. injection of 1 ml PBS. Tumor volume was monitored for the indicated number of days after treatment.

Intraperitoneal tumor model

We confirmed that intraperitoneal (i.p.) injection of SKOV3 cells into 6-week-old female Balb/c nude mice resulted in peritoneally disseminated tumors, ascites, cachexia and death. To assess the efficacy of Hh101, this murine xenograft model was used. Nude mice ($n = 27$) were engrafted i.p. with 2×10^6 SKOV3 cells. HOmMCs were infected for 2 h with MOI = 3 of Hh101 and were used as carriers. After freezing and thawing at 2 h after infection, ~5×10^4 PFU of Hh101 were detected as infectious viruses. To estimate the effect of Hh101 in minimally spread ovarian cancer, HOmMCs (3×10^6 cells) infected with Hh101 were injected i.p. on days 3, 6 and 9. The control groups received 1 ml PBS or Hh101 (5×10^4 PFU ml^{-1}) by i.p. injection on the same days. Mice of each group were followed up to record survival times.

To evaluate the role of Hh101 in more advanced disease, SKOV3 tumors were allowed to grow for 6 days before they were treated. Female Balb/c nude mice (6 weeks old)($n = 10$) were engrafted i.p. with 2×10^6 SKOV3 cells, and this animal group was treated with repeated injection on days 6, 9, 12, 15 and 18. Animals were followed up daily to record survival times.

Localization of virus-associated GFP expression in mice with disseminated ovarian cancer

Female Balb/c nu/nu mice (6 weeks old) were engrafted i.p. with 2×10^6 SKOV3 cells. On day 30, mice were randomized into two cohorts (control, HF-GFP treatment group). The control group received i.p. administration of 1 ml PBS. The HF-GFP treatment group was given 10^7 PFU of HF-GFP i.p. After 24 h, mice were killed and tumors were examined using the Leica M205FA automated fluorescence stereomicroscope with a standard GFP filter set.

To assess the effect of anti-HSV-1 antiserum by using infected carrier cell, we injected control serum or anti-HSV-1 guinea pig antiserum of (500 µl per each mouse, × 1/100 dilution) i.p. into each mouse at 1 h before treatment. HOmMCs were preinfected with HF-GFP (MOI, 3) for 2 h and were washed in PBS. For this experiment, a disseminated ovarian cancer model (1×10^7 SKOV3 cells, i.p.) was established in 6-week-old female Balb/c nu/nu mice. On day 14, mice were randomized qinto control, HF-GFP and HF-GFP-infected HOmMCs groups. The HOmMCs group was treated with 10^7 cells of

HOmMC-infected HF-GFP. Mice were killed after 24 h and the intra-abdominal images were obtained by the fluorescence stereomicroscope. For each experiment, images were captured under identical exposure settings. Overlays were generated using Adobe Photoshop CS software (Adobe Systems, San Jose, CA).

Statistical methods

Data were analyzed using the StatView statistical software package (SAS Institution, Cary, NC). The survival data were analyzed using the Kaplan–Meier method and the log-rank test. Differences in tumor volumes between the treated and control groups were analyzed by the Student's *t*-test. *P*-values <0.05 were considered statistically significant.

Results

Intratumoral Administration of HSV mutants suppresses s.c. tumor growth of human ovarian cancer cells in nude mice

We examined the ability of HF10 to control tumor cell growth in an *in vivo* model. We used an s.c. tumor model, because HF10 is fatal to immunodeficient animals when it is administered intravenously or intraperitoneally. The flanks of Balb/c-nu mice were s.c. injected with 5×10^6 SKOV3 cells. When tumors were palpable (day 8), i.t. injections of PBS or HF10 (1×10^7 PFU) were made on days 8, 10 and 12 for group one, and on days 8, 10, 12, 18, 20 and 22 for group two. Injections (i.t.) with HF10 significantly reduced tumor growth compared with PBS-injected control animals (Figure 2a). Moreover, in group two, complete disappearance of tumors was observed in some animals (Figure 2b). Representative pictures of control and HF10-injected mice are shown (Figure 2c).

In vitro *replication of HSV mutants in MCs, immortalized HOmMCs and SKOV3 cells*

To determine which cell line might be adequate for use as a carrier, we next tested the ability of HF10 and Hh101 to replicate in MCs, immortalized human omentum MCs and in SKOV3 cells. Human MCs may pose considerable advantages as vehicles for oncolytic virotherapy for ovarian cancer. First, MCs can be isolated from patients and grown in culture relatively easily. In addition, if isolated from the same patient that will be treated, autologous transplantation overcomes the difficulties related to immune rejection of the transplanted cells. Cells were infected at MOIs of 3 or 0.03. At MOI of 3, virus titers were ~10-fold higher in HOmMCs than in MCs or SKOV3 cells at 24 h after infection (Figures 3e, f). This correlated with the observation of more extensive and rapid CPEs in HOmMCs than SKOV3 cells (Figure 3c, d). Moreover, viral titers of MCs and SKOV3 cells infected at MOI of 3 and HOmMCs infected at MOI of 0.03 increased equally with time. Virus replication was the most efficient in HomMCs; thus these findings suggested that HOmMCs would be suitable for use as carrier cells.

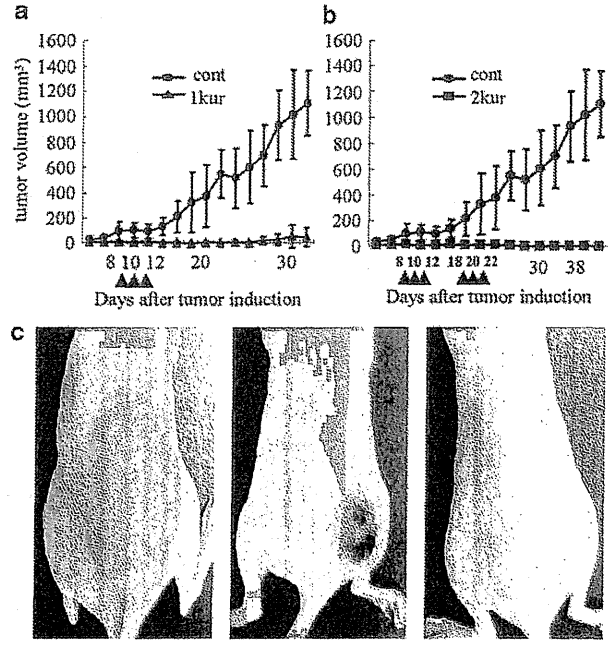

Figure 2 HF10 reduces tumor growth in a subcutaneous (s.c.) ovarian cancer model. (**a**) In all, 5×10^6 SKOV3 cells were s.c. implanted into the flank of 5-week-old nude mice. When s.c. tumors were approximately 10–15 mm in diameter, phosphate-buffered saline (PBS) (control) or 1×10^7 plaque-forming units HF10 were injected intratumorally on days 8, 10 and 12. (**b**) Group two was injected on days 8, 10, 12, 18, 20 and 22. Tumor volume was monitored for the indicated days after treatment ($P<0.01$; control vs HF10 treatment group). Bars represent means + s.e.m. of each group. (**c**) Representative pictures of control (right), group one (middle) and group two (left) at day 30.

In vitro *delivery of HSV using MCs as carrier cells*

We estimated the efficacy of tumor killing caused by virus-loaded carrier cells *in vitro*. To this end, the oncolytic effects of tumor cells cocultured with virus-loaded MCs was compared with direct infection by virus. We administered Hh101- (3×10^5 PFU) or Hh101-infected carrier cells (1×10^5 cells; MOI of 3) to the media of SKOV3 cells. At 24 h after infection, virus titers in the media were 6.3×10^4 PFU ml^{-1} when Hh101-infected carrier cells were administered, and only 2.1×10^2 PFU ml^{-1} when Hh101 virus was administered. Moreover, CPE was observed ~12 h after infection when Hh101-infected carrier cells were administered (Figure 4a), whereas it was observed 24 h after infection with Hh101 virus alone (Figure 4b). CPE was spread more rapidly and extensively in the case of Hh101-infected carrier cells (Figure 4a). Carrier cells therefore supported sufficient viral replication and could contact target cancer cells efficiently.

In vitro *immune evasion by cell-based delivery of HSV*

As the majority of human adults has been exposed to HSV and has anti-HSV antibodies, it is theoretically possible that oncolytic virus would be attenuated by circulating antibodies. To examine the effect of antibodies